

Balloon-Artery Interactions During Stent Placement

A Finite Element Analysis Approach to Pressure, Compliance, and Stent Design as Contributors to Vascular Injury

Campbell Rogers, David Y. Tseng, James C. Squire, Elazer R. Edelman

Abstract—Endovascular stents expand the arterial lumen more than balloon angioplasty and reduce rates of restenosis after coronary angioplasty in selected patients. Understanding the factors involved in vascular injury imposed during stent deployment may allow optimization of stent design and stent-placement protocols so as to limit vascular injury and perhaps reduce restenosis. Addressing the hypothesis that a previously undescribed mechanism of vascular injury during stent deployment is balloon-artery interaction, we have used finite element analysis to model how balloon-artery contact stress and area depend on stent-strut geometry, balloon compliance, and inflation pressure. We also examined superficial injury during deployment of stents of varied design in vivo and in a phantom model ex vivo to show that balloon-induced damage can be modulated by altering stent design. Our results show that higher inflation pressures, wider stent-strut openings, and more compliant balloon materials cause markedly larger surface-contact areas and contact stresses between stent struts. Appreciating that the contact stress and contact area are functions of placement pressure, stent geometry, and balloon compliance may help direct development of novel stent designs and stent-deployment protocols so as to minimize vascular injury during stenting and perhaps to optimize long-term outcomes. (*Circ Res.* 1999;84:378-383.)

Key Words: stent ■ restenosis ■ vascular injury ■ balloon ■ finite element analysis

Endovascular stents expand the arterial lumen more than balloon angioplasty and reduce rates of restenosis after coronary angioplasty in selected patients.^{1,2} However, the deep vascular trauma imposed by stent struts^{3,4} produces more abundant intimal hyperplasia than balloon angioplasty in experimental animals⁵⁻⁷ and in humans.^{1,2,8} Furthermore, understanding the practical elements that underlie in-stent restenosis is made all the more crucial in light of the failure to date to identify successful treatments for established in-stent restenosis. Understanding the factors involved in vascular injury imposed during stent deployment might allow optimization of stent design (eg, stent-strut geometry and stent material) and stent-placement protocols (eg, balloon selection and inflation pressure) so as to limit vascular injury and perhaps reduce restenosis.

In addition to mechanical factors such as focal deep injury from struts and overall arterial strain, which may play important roles in provoking in-stent restenosis, we have recently reported that stent deployment causes partial denudation of the endothelium in a pattern unique to each stent configuration, suggesting balloon-related injury.⁹ Assuming that endothelial denudation is a marker of the distribution of

interstrut vascular injury caused during stent deployment, we now describe studies aimed at elaborating the mechanisms that underlie injury patterns during stenting. Addressing the hypothesis that the mechanism of endothelial cell denudation and therefore interstrut injury during stent deployment is balloon-artery interaction, we have examined damage to endothelial cells during deployment of stents of varied design in vivo and the balloon-stent inflation process and balloon extrusion between stent strut openings in a phantom model ex vivo. Finally, we used finite element analysis (FEA) to model how balloon-artery contact stress and area depend on stent-strut geometry, balloon compliance, and inflation pressure. Understanding more fully the mechanism of interactions among balloon, artery, and stent may help limit neointimal thickening after stenting.

Materials and Methods

In Vivo Analysis of Endothelial Cell Denudation

Balloon-expandable stainless-steel stents were mounted on 3-mm angioplasty balloons (Advanced Cardiovascular Systems) and expanded at 8 atm over 20 s in the iliac arteries (2.5 to 2.75 mm)⁶ of New Zealand White rabbits (3.0 to 3.5 kg) treated with aspirin and

Received August 7, 1998; accepted December 4, 1998.

From the Cardiac Catheterization Laboratory and Coronary Care Unit, Cardiovascular Division, Brigham and Women's Hospital, Harvard Medical School, Boston, Mass, and Harvard-MIT Division of Health Science and Technology, Massachusetts Institute of Technology, Cambridge, Mass.

Presented at the 23rd Annual Meeting of the Society for Biomaterials, New Orleans, La, April 30–May 4, 1997, and the 70th Scientific Sessions of the American Heart Association, Orlando, Fla, November 9–12, 1997, and published in abstract form (*Circulation*. 1997;96[suppl I]:I-402).

Correspondence to Campbell Rogers, MD, Cardiovascular Division, Brigham and Women's Hospital, 75 Francis St, Boston, MA 02115. E-mail cdrogers@bics.bwh.harvard.edu

© 1999 American Heart Association, Inc.

Circulation Research is available at <http://www.circresaha.org>

heparin as described previously.¹⁰ Two distinct stent configurations,¹⁰ a slotted tube and a series of connected corrugated rings, were used. The stent struts were constructed from identical material and had the same strut thickness and surface area. Arteries (n=8 for each stent type) were harvested 1 hour after deployment, en face endothelial staining was performed using a modified Hautchen preparation, the area of intact endothelium remaining between stent struts was measured using computerized digital morphometry,⁹ and the percentage area of endothelial denudation was calculated.

Ex Vivo Visualization and Analysis of Balloon-Artery Interactions

To visualize how stent and artery interact during the stent-balloon inflation process and perhaps explain the observed patterns of in vivo endothelial injury, we used a glass-tube arterial phantom model. A glass tube (Pyrex, ID 2.75 mm, 10 cm long) was filled with water colored with black India ink and placed under a stereomicroscope (model M5A; Wild). Stents of corrugated-ring or slotted-tube design were mounted on 3-mm angioplasty balloons (Advanced Cardiovascular Systems/Guidant), and each was inserted into the center portion of a glass tube. After positioning the stent-mounted balloon, colored water was injected into the glass tube, and air bubbles were removed. The balloon was then inflated to 8 atm over 20 s. Magnified video images were recorded before inflation and at 8 atm pressure.

Finite Element Analysis

To study how individual components of the balloon-artery interaction may affect associated contact stress and thereby vascular injury, we developed an FEA model, using Automatic Dynamic Incremental Nonlinear Analysis software (ADINA 7.0, ADINA R&D, Inc) on a dedicated workstation (Silicon Graphics). Our model included input of the following: individual stent-strut width and thickness and interstrut distances of the corrugated-ring and slotted-tube stents described above, Young's modulus and Poisson's ratio for the balloon material, arterial-wall thickness, Young's modulus (circumferential) and Poisson's ratio for the artery, and pressure loaded into the balloon.

The relationship of balloon-artery contact stress and contact area with the distance between 2 adjacent stent struts, balloon materials, and inflation pressure was analyzed by a 2-dimensional FEA model. The FEA model used in this analysis included both displacement and pressure loading to represent arterial displacement and balloon extrusion between struts, respectively. The model assumed the following: (1) a balloon membrane with no thickness; (2) frictionless contact between balloon surface and artery; (3) no slip between stent struts and luminal surface; and (4) no other substrates, such as blood, present between the balloon surface and the arterial wall. The distance between balloon and luminal surfaces before inflation was set as the same as stent-strut thickness (100 μm). Eight-node 2-dimensional solid plane-strain elements and 2-node isobeam plane-strain elements were used for arterial and balloon surface, respectively. Constant step-time functions were used to control artery displacement and balloon extrusion between struts during analysis. The correlations of maximum contact stress and contact area with balloon pressure and the distance between adjacent stent struts at different Young's moduli of balloon materials were analyzed.

Dimensions of the slotted-tube stent design were measured. Young's modulus (circumferential) and Poisson's ratio for the arterial wall, based on previously published studies, were 100 kPa and 0.27, respectively.^{11,12} Arterial-wall thickness was input as 500 μm . The Young's moduli of balloon materials were measured on a strain-stress measurement instrument (Instron) with a 50-kg load. The Young's modulus was 2.58×10^4 kPa for a compliant balloon (LEAP, Boston Scientific Co/Scimed) and 7.03×10^5 kPa for a semicompliant balloon (TRIAD, Boston Scientific Co). Because of difficulty measuring the Young's moduli of noncompliant balloon materials, this value was estimated on the basis of material properties. For FEA, 3 values for Young's modulus of a balloon within the range of the measured values were chosen (1.38×10^6 kPa, 6.9×10^5

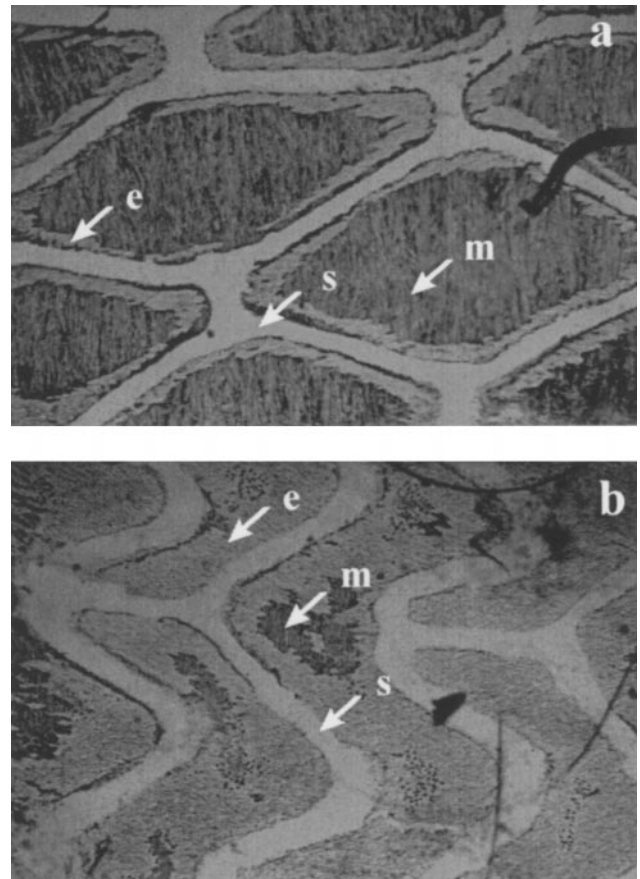


Figure 1. En face photomicrographs show partially denuded luminal surfaces of rabbit iliac arteries 1 hour after balloon expansion of a slotted-tube design (a) or corrugated-ring design (b) stent. Stent wire locations (s), remnant endothelial cells (e), and medial smooth muscle cells (m) are indicated. Original magnification, $\times 40$.

kPa, and 3.45×10^5 kPa) to give a ratio of 2:1:0.5 for low-compliant, semicompliant, and compliant balloons, respectively. Poisson's ratio for the balloons was chosen as 0.30.¹³ The arterial displacement was based on the assumption that a 3.0-mm-ID vessel was expanded to 3.1 mm ID.

Statistical Analysis

All data are presented as mean \pm SE. Comparison of endothelial denudation of slotted-tube and corrugated-ring stents used an unpaired Student *t* test. Probability values < 0.05 were considered significant.

Results

In Vivo Analysis of Endothelial Cell Denudation

Denudation of endothelial cells during stent expansion, as a marker of balloon-induced damage, was determined by en face staining 1 hour after stent placement in rabbit iliac arteries. Stents of slotted-tube and corrugated-ring designs were compared. Although endothelial denudation occurred at the center of each interstrut opening (Figure 1), less endothelium was denuded after deployment of corrugated-ring design stents ($42.6 \pm 4.6\%$, n=8) than after slotted-tube design stents ($63.0 \pm 4.3\%$, n=8, $P < 0.01$, Figure 2).

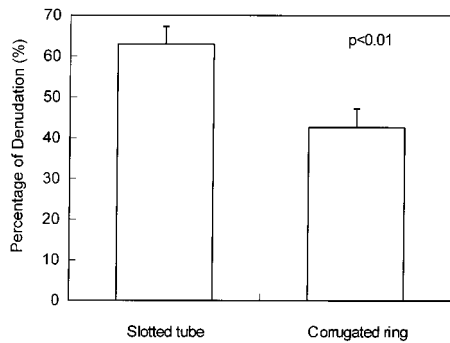


Figure 2. Bar graph shows the percentage of luminal surface denuded of endothelium 1 hour after balloon expansion of slotted-tube design or corrugated-ring design stents in rabbit iliac arteries. Data are mean+SE.

Ex Vivo Visualization and Analysis of Balloon-Artery Interactions

To examine possible mechanisms of balloon-artery interactions during stent deployment, the stent-balloon inflation process was visualized inside a glass-tube arterial model. The inflation process included 2 stages. The first stage was gradual inflation of the balloon and stent until the stent just made contact with the luminal surface of the glass tubing. The second stage, as balloon pressure continued to increase, included portions of the balloon being extruded between stent struts to make contact with the luminal surface of the glass tube, after the stent had contacted the glass tubing. Digital images of balloon extruded between stent-strut openings were recorded for slotted-tube and corrugated-ring design stents (Figure 3). The pattern of the balloon-tubing contact identified in this model was identical to the pattern of endothelial-cell denudation identified from en face staining after in vivo stent deployment (Figure 1).

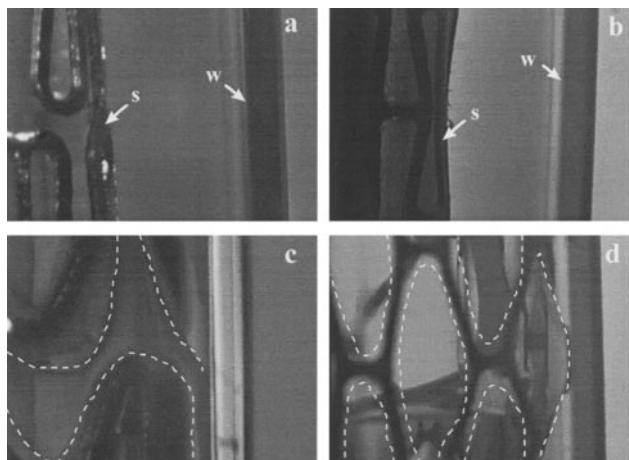


Figure 3. Magnified digital images show balloon extrusion between stent struts (s) during inflation within a glass-walled tube (w). a, Balloon and corrugated-ring stent before expansion; b, balloon and slotted-tube stent before expansion; c, balloon extruded between corrugated-ring stent struts at 8 atm pressure; d, balloon extruded between slotted-tube stent struts at 8 atm pressure. Dashed lines indicate the contact area between balloon and glass tube. Original magnification, $\times 25$.

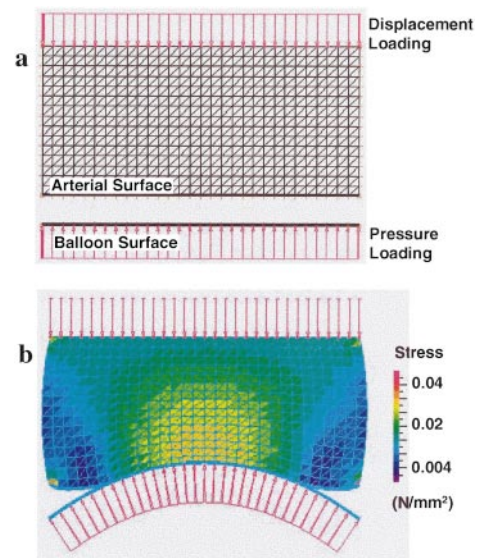


Figure 4. Balloon surface displacement and contact stress in 2-dimensional FEA. a, Schematic diagram of model before analysis. b, Displacement of arterial and balloon surface and associated contact stress in analysis with input values of 0.96 mm interstrut distance, 0.05 mm displacement loading, and 8 atm pressure loading.

Finite Element Analysis

FEA was used to investigate in a continuous fashion independent effects of distance between stent struts, balloon-material properties, and balloon inflation pressures on balloon-artery surface stress and contact area. In the 2-dimensional FEA contact model with 0.05 mm displacement and 8 atm deployment pressure, the balloon-artery displacement (including arterial displacement and balloon extrusion) and balloon-artery interactions were modeled (Figure 4).

The correlations between balloon-artery surface stress or contact area and the distance between 2 adjacent stent struts, the placement pressure, and different balloon materials, were analyzed. With constant interstrut distance and balloon compliance, the effective surface stress increased with deployment pressure (Figure 5a) and reached a maximum at the center of the intrastrut opening primarily caused by contact between artery and balloon. Maximum contact stress rose exponentially with deployment pressure in the range of 12 to 18 atm pressure (Figure 5b). Examining how balloon compliance affects surface stress in the elastic region of balloon materials, we found that normalized contact area between balloon and artery (Figure 6a) and maximum contact stress (Figure 6b) also increased with interstrut distance and balloon compliance.

Discussion

How an artery is injured experimentally or clinically may be a critical determinant of the biological events that ensue. We now report a new approach to quantifying the unique forces applied to vessel walls during a particular form of vascular injury, endovascular stent placement. To date, stent-induced arterial injury has been considered to be limited to the sites of stent struts, where depending on stent design and size, deep

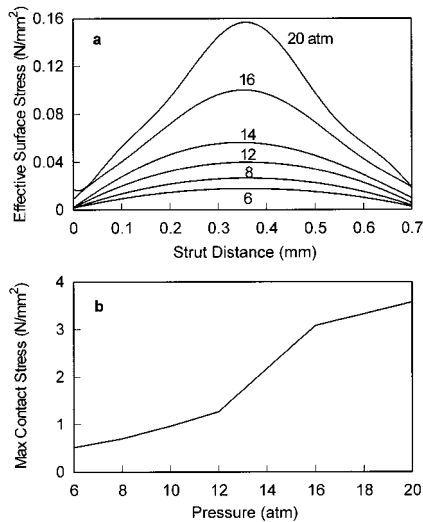


Figure 5. Line graphs from 2-dimensional contact analysis show the relationships between stent expansion pressure and effective surface-contact stress over the distance between 2 adjacent stent struts (a) or maximum contact stress (b). Young’s modulus for the balloon is 6.90×10^5 kPa; Young’s modulus for the artery, 100 kPa; and total interstrut distance, 0.96 mm.

wall laceration translates into greater vascular responses.^{3,4,10,14} At the same time, with current clinical stent-deployment techniques including balloon predilation, stent expansion at moderate balloon pressures, and postdilation at significantly higher balloon pressures to ensure that all stent struts are fully expanded and abutting the arterial wall,¹⁵ elements of stent implantation such as balloon inflation pressure, balloon material, and arterial stretching, independent of stent design, have taken on tremendous importance in clinical practice. Our report now provides data for the first time that suggest how these various elements may contribute

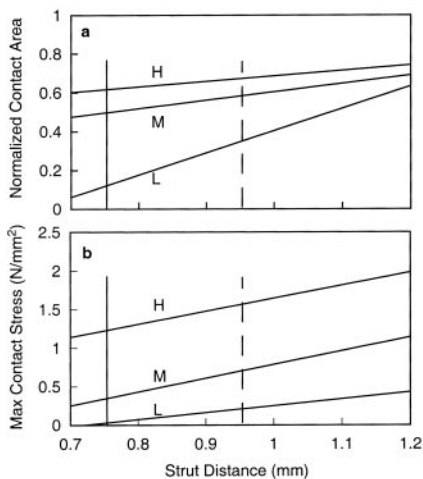


Figure 6. Line graphs from 2-dimensional contact analysis show the relationships between normalized contact area (a) or maximum contact stress (b) and interstrut distance or balloon-material compliance. Expansion pressure, 8 atm; Young’s moduli for low-compliance balloon (L) is 1.38×10^6 kPa; for semi-compliant balloon (M), 6.90×10^5 kPa; and for high-compliance balloon (H), 3.45×10^5 kPa. The measured interstrut distances for the 2 stent designs are indicated. Solid line indicates corrugated-ring stent; dashed line, slotted-tube stent.

to vascular injury. In particular, in vivo and bench-top stent expansion demonstrate contact of the expansion balloon with the vessel wall between stent struts, and FEA demonstrates that small alterations in inflation pressure, balloon material, or stent design can each have large effects on the area of balloon-artery contact and the stress applied by the balloon to the arterial wall.

Sites of Injury

In addition to the deep injury associated with stent expansion, more superficial vascular injury occurs during stent expansion in areas removed from stent struts themselves.⁹ First, asking whether the shape of the areas bounded by stent struts influenced the degree of damage, we altered stent design so as to alter this shape. Using stents of which the total surface area and strut thickness were the same but the geometric configuration different, and using endothelial loss as a marker for superficial injury, we demonstrated that the stent design in which the struts created a more complex and closed area (corrugated-ring design) permitted 33% less injury in the spaces bounded by each strut than did the stent design in which the interstrut areas were more simple and open in shape (slotted-tube design). In contrast, in the absence of a stent, balloon-artery contact during an angioplasty covers 100% of the luminal surface, and one would anticipate that denudation would encompass 100% of the arterial surface.

To visualize balloon-“vessel” interactions at the sites of superficial endothelial injury, we constructed a phantom model using a glass tube in lieu of an artery. During inflation, after the stent struts had contacted the vessel wall, further increases in balloon pressure led to the balloon material being extruded through the openings bounded by stent struts. Balloon extrusion was sufficient to cause direct contact between balloon and glass tube, and the shape of this contact area matched the area of vascular injury previously identified in vivo. For any given stent design, as balloon pressure rises, the area of balloon-artery contact would also rise but would reach a limit of <100% of the arterial surface, always leaving a cuff of surface directly adjacent to the struts free from contact.

Sources of Injury

We next sought to examine what force and stress would be transmitted to the arterial wall via balloon-artery contact. Using FEA, we constructed a model to determine the force applied by a balloon to the arterial surface with boundary conditions chosen to mimic a balloon extruding between 2 stent struts. From this surface force, we modeled the amount of stress developed within the arterial wall. The input variables we studied were interstrut distance (reflecting stent design) and balloon expansion pressure and compliance. FEA showed that as interstrut distance grew, so too did the maximum surface-contact stress and normalized contact area (Figure 6). This again confirmed that increasing the geometric complexity of stent design, or increasing the number of struts for a given arterial surface area, would reduce the surface-contact stress and contact area imparted by the balloon to the artery during stent deployment.

Holding interstrut distance and balloon compliance constant, FEA demonstrated that maximum surface-contact force grew in a nonlinear fashion as balloon pressure climbed (Figure 5). There was a rapid rise in predicted maximum arterial-surface force between 12 and 18 atm followed by a plateau at higher pressures. This finding is of particular importance, as the pressures chosen to dilate stents in clinical practice range between 12 and 18 atm.¹⁵ Of note, some data suggest that high stent postdilation pressures may be correlated with greater restenosis.¹⁶ Potential adverse ramifications of high pressure dilation after stent deployment, particularly with stents imbued with enhanced thromboresistance,¹⁷ will need to be addressed.

Finally, FEA demonstrated that maximum surface-contact stress and normalized contact area grew as balloon compliance increased, reflecting greater degrees of balloon extrusion between struts (Figure 6). There was a 15-fold difference in maximum surface-contact stress between a compliant balloon and a semicompliant balloon at 8 atm. This finding pertains to both stent-deployment balloons and postdilation balloons, indicating that lower balloon compliance will lead to lower arterial-wall stress and perhaps less vascular injury.

Surface-Contact Force and Vascular Injury

Balloon-Artery Interactions

Injury to endothelial cells and the underlying smooth muscle cells produces experimental neointimal hyperplasia.^{18–21} While denudation of endothelial cells alone produces mild neointimal thickening,²² more substantial neointimal hyperplasia requires direct injury to medial smooth muscle cells.^{23,24} In stented arteries, a correlation exists between the depth of arterial injury and the extent of intimal thickening.^{3,4,10} In humans, higher inflation pressures and larger balloon sizes may also cause greater neointimal hyperplasia.^{16,25–27} Possible mechanisms whereby balloon-induced stress may be a determinant of restenosis include effects of either transient or cyclical stress on vascular smooth muscle cells.^{24,28–31} Also, acute luminal stretching at the time of angioplasty has been shown to be an accurate predictor of later luminal loss.^{32–35}

Superficial injury during stent deployment is the result of balloon and artery vessel wall interactions. During stent placement, the balloon and arterial vessel interactions include 2 opposite elements, balloon extrusion and arterial displacement, as both balloon surface and arterial wall are not totally rigid. If we assumed total rigidity of artery, the balloon would extrude. On the other hand, if we assumed total rigidity (low compliance) of the balloon, the artery would prolapse into the stent-strut interstices during and after balloon expansion. Because neither vessel nor balloon is totally rigid, we included both arterial displacement and balloon deformation in FEA modeling. To represent arterial displacement and balloon extrusion, displacement and pressure loadings were used. The model assumed this highly nonlinear contact as a planar-contact problem. The solution procedures to address contact problems can be found in previous studies.^{36,37}

Our data suggest 3 ways to alter contact stress. First, the contact-stress distribution at the balloon-artery interface is a function of stent-placement pressure. In the elastic region of

the balloon material, the maximum surface-contact force increased with increasing deployment pressure. Increasing deployment pressure from 4 to 16 atm, the effective surface stress increased in a nonlinear fashion and reached a maximum in the center of the intrastrut opening. Second, contact area and stress created at the balloon-artery interface are functions of stent geometry. The greater the distance between 2 adjacent stent struts, the more the balloon extrusion, and the greater arterial displacement during and after expansion. The normalized contact area and maximum contact force increased with increasing interstrut distance. Third, balloon-material properties affect the contact area and surface-contact stress. Balloon material with higher compliance would allow more balloon extrusion and more arterial displacement between struts at any given pressure. As the compliance of balloon material chosen for FEA modeling fell, the normalized contact area and maximum contact stress both decreased.

Permanent mechanical stress imposed by stent struts and strain imposed by stent deformation even after balloon withdrawal could also contribute to superficial and deep arterial injury. However, the stress and strain caused by stent deformation after balloon removal are actually lower at the center of interstrut openings than that at the stent struts themselves (data not shown). The mechanical tearing or scraping imposed by stent struts as they traverse the arterial surface during expansion might also contribute to superficial injury.³⁸ Another contributing factor might be fluid-shear stress caused by blood confined to the closed space between balloon surface, stent strut, and arterial luminal wall, a mechanism that distributes surface stress equally over the entire interstrut area. However, none of these mechanisms are consistent with the pattern of endothelial denudation observed.

Study Limitations

This study constructs a theoretical basis for measuring balloon-artery interactions during stent deployment. Input parameters for physical arterial-wall characteristics were taken from published data, and values for diseased arteries may differ. Specifically, more rigid diseased arteries undergoing more substantial degrees of dilation would demonstrate much greater surface-contact stresses. Nevertheless, the relative effects of varying chosen variables such as balloon material, stent design, or inflation pressure are not likely to change. We have not examined late in vivo ramifications of varying balloon-related vascular injury through altering stent design, balloon material, or inflation pressure. Stent expansion also imposes injury in the direct vicinity of stent struts not included in our FEA model. Developing techniques for 3-dimensional FEA analysis and for studying stress analysis in vivo³⁹ will allow extension of this model from comparing effects of different parameters in a relative fashion to identifying optimal design parameters.

Implications

Balloon-artery interactions during stent placement were observed and verified by in vivo and in vitro visualization and modeled by FEA. These interactions may contribute to vascular injury during stent placement. The acute contact of balloon with artery wall may have direct impact on vascular injury above and beyond that caused by balloon angioplasty

alone and explain in part the greater degree of neointimal thickening seen after stent implantation in experimental animals⁵⁻⁷ and humans.^{1,2,8} Appreciating that the contact stress and contact area are functions of placement pressure, stent geometry, and balloon compliance may help direct development of novel stent designs and stent-deployment protocols so as to minimize vascular injury and optimizing long-term outcomes.

Acknowledgments

This work was supported by American Heart Association National Center Grant 95004400 (to C.R.), National Institutes of Health Grants HL03104 (to C.R.) and GM/HL 49039 (to E.R.E.), and grants from the Burroughs Wellcome Fund for Experimental Therapeutics and the Whitaker Foundation (both to E.R.E.). We are grateful to Philip Seifert for technical assistance.

References

- Serruys PW, de Jaegere P, Kiemeneij F, Macaya C, Rutsch W, Heyndrickx G, Emanuelsson H, Marco J, Legrand V, Materne P, Belardi J, Sijwart U, Colombo A, Goy J, van den Heuvel P, Delcan J, Morel M. A comparison of balloon-expandable-stent implantation with balloon angioplasty in patients with coronary artery disease: Benestent Study Group. *N Engl J Med*. 1994;331:489-495.
- Fischman DL, Leon MB, Baim DS, Schatz RA, Savage MP, Penn IM, Detre K, Veltri L, Ricci DR, Nobuyoshi M, Cleman MW, Heuser RR, Almond D, Teirstein PS, Fish RD, Colombo A, Brinker J, Moses J, Shalnovich A, Hirshfeld J, Bailey S, Ellis S, Rake R, Goldberg S. A randomized comparison of coronary artery-stent placement and balloon angioplasty in the treatment of coronary artery disease. *N Engl J Med*. 1994;331:496-501.
- Schwartz RS, Huber KC, Murphy JG, Edwards WD, Camrud AR, Vlietstra RE, Holmes DR. Restenosis and proportional neointimal response to coronary artery injury: results in a porcine model. *J Am Coll Cardiol*. 1992;19:267-274.
- Schwartz RS, Holmes DH, Topol EJ. The restenosis paradigm revisited: an alternative proposal for cellular mechanisms. *J Am Coll Cardiol*. 1992;20:1284-1293.
- Karas SP, Gravanis MB, Santoian EC, Robinson KA, Anderberg KA, King SB III. Coronary intimal proliferation after balloon injury and stenting in swine: an animal model of restenosis. *J Am Coll Cardiol*. 1992;20:467-474.
- Rogers C, Karnovsky MJ, Edelman ER. Inhibition of experimental neointimal hyperplasia and thrombosis depends on the type of vascular injury and the site of drug administration. *Circulation*. 1993;88:1215-1221.
- Hanke H, Kamenz J, Hassenstein S, Oberhoff M, Haase KK, Baumbach A, Betz E, Karsch KR. Prolonged proliferative response of smooth muscle cells after experimental intravascular stenting. *Eur Heart J*. 1995; 16:785-793.
- Topol EJ. Caveats about elective coronary stenting. *N Engl J Med*. 1994;331:539-541.
- Rogers C, Parikh S, Seifert P, Edelman ER. Endogenous cell seeding: remnant endothelium after stenting enhances vascular repair. *Circulation*. 1996;94:2909-2914.
- Rogers C, Edelman ER. Endovascular stent design dictates experimental restenosis and thrombosis. *Circulation*. 1995;91:2995-3001.
- Patel DJ, Janicki JS, Carew TE. Static anisotropic elastic properties of the aorta in living dogs. *Circ Res*. 1969;25:765-779.
- Patel DJ, Janicki JS. Static elastic properties of the left coronary circumflex artery and the common carotid artery in dogs. *Circ Res*. 1970; 27:149-158.
- Seymour RB, Carraher CE. *Polymer Chemistry: An Introduction*. New York, NY: Marcel Dekker, Inc. 1992.
- Barth KH, Virmani R, Froelich J, Takeda T, Lossef SV, Newsome J, Jones R, Lindisch D. Paired comparison of vascular wall reactions to Palmaz stents, Strecker tantalum stents, and Wallstents in canine iliac and femoral arteries. *Circulation*. 1996;93:2161-2169.
- Colombo A, Hall P, Nakamura S, Almagor Y, Maiello L, Martini G, Gaglione A, Goldberg SL, Tobis JM. Intracoronary stenting without anticoagulation accomplished with intravascular ultrasound guidance. *Circulation*. 1995;91:1676-1688.
- Savage MP, Fischman DL, Douglas JS Jr, Pepine CJ, Werner JA, Bailey SR, Rake R, Goldberg S. The dark side of high pressure stent deployment. *J Am Coll Cardiol*. 1997;29:368A. Abstract.
- Serruys PW, Emanuelsson H, van der Giessen W, Lunn AC, Kiemeneij F, Macaya C, Rutsch W, Heyndrickx G, Suryapranata H, Legrand V, Goy JJ, Materne P, Bonnier H, Morice MC, Fajadet J, Belardi J, Colombo A, Garcia E, Ruygrok P, de Jaegere P, Morel MA. Heparin-coated Palmaz-Schatz stents in human coronary arteries: early outcome of the Benestent-II Pilot Study. *Circulation*. 1996;93:412-22.
- Baumgartner HR, Spaet TH. Endothelial replacement in rabbit arteries. *Fed Proc*. 1970;29:710. Abstract.
- Fishman JA, Ryan GB, Karnovsky MJ. Endothelial regeneration in the rat carotid artery and the significance of endothelial denudation in the pathogenesis of myointimal thickening. *Lab Invest*. 1975;32:339-351.
- Stemmerman MB, Spaet TH, Pitlick F, Cintron J, Lejniak I, Tiell ML. Intimal healing: the pattern of reendothelialization and intimal thickening. *Am J Pathol*. 1977;87:125-142.
- Clowes AW, Clowes MM. Kinetics of cell proliferation after arterial injury. I. Smooth muscle cell growth in the absence of endothelium. *Lab Invest*. 1983;49:327-335.
- Fingerle J, Au T, Clowes AW, Reidy MA. Intimal lesion formation in rat carotid arteries after endothelial denudation in the absence of medial injury. *Arteriosclerosis*. 1990;10:1082-1087.
- Walker LN, Ramsay MM, Bowyer DE. Endothelial healing following defined injury to rabbit aorta: depth of injury and mode of repair. *Arteriosclerosis*. 1983;47:123-130.
- Clowes AW, Clowes MM, Fingerle J, Reidy MA. Kinetics of cellular proliferation after arterial injury. V. Role of acute distension in the induction of smooth muscle proliferation. *Lab Invest*. 1989;70:360-364.
- Sarembock IJ, LaVeau PJ, Sigal SL, Timms I, Sussman J, Haudenschild C, Ezekowitz MD. Influence of inflation pressure and balloon size on the development of intimal hyperplasia after balloon angioplasty: a study in the atherosclerotic rabbit. *Circulation*. 1989;80:1029-1040.
- Hirshfeld JW, Schwartz JS, Jugo R, Macdonald RG, Goldberg S, Savage MP, Bass TA, Vetrovec G, Cowley M, Taussig AS, Whitworth HB, Margolis JR, Hill JA, Pepine CJ. Restenosis after coronary angioplasty: a multivariate statistical model to relate lesion and procedure variables to restenosis. *J Am Coll Cardiol*. 1991;18:647-656.
- Roubin GS, Douglas JS Jr, King SB III. Influence of balloon size on initial success, acute complications, and restenosis after percutaneous transluminal coronary angioplasty. *Circulation*. 1988;78:557-565.
- Kulik TJ, Rothman A, Glennon ET, Underwood RH. Stretching vascular smooth muscle causes inositol phosphates turnover. *Circulation*. 1989; 80(suppl II):II-198.
- Leung DY, Glagov S, Mathews MB. Cyclic stretching stimulates synthesis of matrix components by arterial smooth muscle cells in vitro. *Science*. 1975;191:475-477.
- Cheng GC, Libby P, Grodzinsky AJ, Lee RT. Induction of DNA synthesis by a single transient mechanical stimulus of human vascular smooth muscle cells: role of fibroblast growth factor-2. *Circulation*. 1996;93:99-105.
- Buck RC. Behavior of vascular smooth muscle cells during repeated stretching of the substratum in vitro. *Atherosclerosis*. 1983;46:217-223.
- Kuntz RE, Safian RD, Carozza JP, Fishman RF, Mansour M, Baim DS. The importance of acute luminal diameter in determining restenosis after coronary atherectomy or stenting. *Circulation*. 1992;86:1827-1835.
- Post MJ, Borst C, Kuntz RE. The relative importance of arterial remodeling compared with intimal hyperplasia in lumen renarrowing after balloon angioplasty. *Circulation*. 1994;89:2816-2821.
- Anderson HR, Maeng M, Thorwest M, Falk E. Remodeling rather than neointimal formation explains luminal narrowing after deep vessel wall injury. *Circulation*. 1996;93:1716-1724.
- Kakuta T, Currier JW, Haudenschild CC, Ryan TJ, Faxon DP. Differences in compensatory vessel enlargement, not intimal formation, account for restenosis after angioplasty in the hypercholesterolemic rabbit model. *Circulation*. 1994;89:2809-2815.
- Bathe K, Chaudhary A. A solution method for planar and axisymmetric contact problems. *Int J Numer Methods Eng*. 1985;21:65-88.
- Bathe KJ. *Finite Element Procedures*. Englewood Cliffs, NJ: Prentice Hall; 1996.
- Van Belle E, Tio FO, Couffinal T, Maillard L, Passeri J, Isner JM. Stent endothelialization: time course, impact of local catheter delivery, feasibility of recombinant protein administration, and response to cytokine administration. *Circulation*. 1995;95:438-448.
- Squire JC, Rogers C, Edelman ER. Stent geometry during inflation influences later restenosis. *Circulation*. 1996;94(suppl I):I-259. Abstract.